Cleavage of Symmetric Immobile DNA Junctions by *Escherichia coli* RuvC†

Ruojie Sha,‡ Hiroshi Iwasaki,*,§,|| Furong Liu,§ Hideo Shinagawa,§ and Nadrian C. Seeman*,‡,§

Department of Chemistry, New York University, New York, New York 10003, and Department of Molecular Microbiology, Research Institute for Microbial Diseases, Osaka University, and PRESTO, JST, 3-1 Yamadaoka, Suita, Osaka 565-0871, Japan

Received May 5, 2000; Revised Manuscript Received July 27, 2000

ABSTRACT: The Holliday junction is a key DNA intermediate in the process of genetic recombination. It consists of two double-helical domains composed of homologous strands that flank a branch point; two of the strands are roughly helical, and two form the crossover between the helices. RuvC is a Holliday junction resolvase that cleaves the helical strands at a symmetric sequence, leading to the production of two recombinant molecules. We have determined the position of the cleavage site relative to the crossover point by the use of symmetric immobile junctions; these are DNA molecules containing two crossover points, one held immobile by sequence asymmetry and the second a symmetric sequence, but held immobile by torsional coupling to the first junction. We have built five symmetric immobile junctions, in which the tetranucleotide recognition site is moved stepwise relative to the branch point. We have used kinetic analysis of catalysis, gel retardation, and hydroxyl radical hypersensitivity to analyze this system. We conclude that the internucleotide linkage one position 3′ to the crossover point is the favored site of cleavage.

Recombination is a process that promotes genetic diversity within all species. The basic feature of recombination is the interaction of two pieces of DNA to yield new genetic material, which may incorporate information from both interacting molecules. The resulting DNA may contain insertions, deletions, changes of sequence, rearrangements, or exchanges of flanking markers. The Holliday junction (*1*) is a central intermediate in recombination, known to participate in site-specific recombination (*2*−*4*) and thought to be involved in homologous recombination as well (*5*). This is a four-stranded molecule containing a branch point surrounded by four double-helical arms. In naturally occurring systems, the sequence flanking the branch point of the Holliday junction is 2-fold symmetric (homologous), enabling the branch point to migrate. Most characterization of Holliday junction-like molecules has been performed with immobile branched junctions (for reviews, see refs *6* and *7*), whose sequence symmetry prevents branch migration (*8*).

The role of the Holliday junction in recombination is illustrated in Figure 1. Six stages are shown, with five steps between them. First is junction formation, which requires the involvement of proteins (reviewed in ref *9*), followed by branch migration (reviewed in ref *10*). In the third, optional, step, crossover isomerization, the crossover strands and the helical strands exchange roles; this process is known

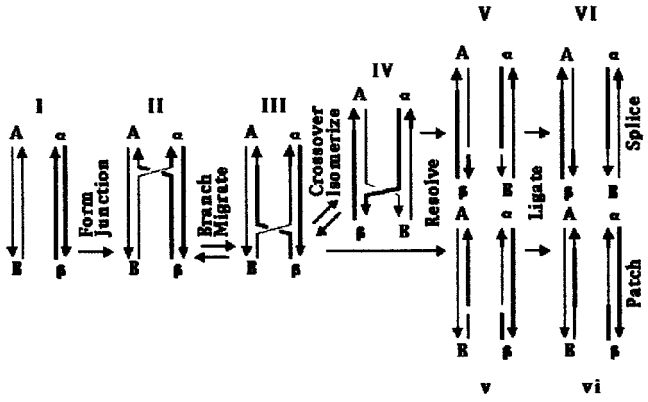

FIGURE 1: Formation and resolution of the Holliday structure in genetic recombination. The process proceeds from left to right. Each stage is labeled with capital or small Roman numerals. In stage **I**, two homologous DNA double helices align. The two strands of each duplex are shown as two pairs of lines terminated by arrowheads, indicating the 3′ ends. Strands are distinguished by their thickness. Each homologous region carries a flanking marker, A and B on the left and α and β on the right. After the first step, the homologous pairs have formed a Holliday intermediate **II**. The two crossover strands are composite strands with both a thick and a thin portion formed through any of a number of possibilities. A parallel Holliday junction is shown. Its homologous sequence symmetry permits it to undergo branch migration; movement as indicated results in structure **III**. The Holliday intermediate may or may not undergo crossover isomerization to produce structure **IV**, which switches the crossover and noncrossover strands. If crossover isomerization occurs an odd number of times, resolution by cleavage of the crossover strands yields structure **V**, but structure **v** results from an even number of switches before cleavage. Ligation of **v** generates a patch recombinant, **vi**, and ligation of **VI** yields a splice recombinant. Cleavage of the noncrossover strands leads to opposite products.

† This research has been supported by Grants GM-29554 from the National Institute of General Medical Sciences, N00014-98-1-0093 from the Office of Naval Research, NSF-CCR-97-25021 from the National Science Foundation/DARPA, and F30602-98-C-0148 from the Information Directorate of the Air Force Research Laboratory located in Rome, NY, to N.C.S. and by Grants-in Aid for Scientific Research on Priority Areas from the Ministry of Education, Science, Sports and Culture of Japan to H.S.

* To whom correspondence should be addressed. N.C.S.: e-mail, ned.seeman@nyu.edu; phone, (212) 998-8395; fax, (212) 260-7905. H.I.: e-mail, iwasaki@biken.osaka-u.ac.jp; phone, 81-6-6879-8319; fax, 81-6-6879-8320.

‡ New York University.

§ Osaka University.

|| PRESTO.

10.1021/bi001037z CCC: $19.00
Published on Web 08/31/2000

to be spontaneous (*11*), and the free energy differences between asymmetric flanking sequences (*12*) tend to be larger than those between symmetric flanking sequences (*13*). In the fourth step, the junction is cleaved to linear duplex by a resolvase, followed by ligation to seal the nicks introduced by resolution. The products are either splice recombinants in which flanking markers are exchanged or patch recombinants, which can lead to gene conversion. Cleavage is shown on the crossover strands, which is true for endonuclease VII (*14*); however, for RuvC resolvase, the cuts are on the noncrossover strands, resulting in the opposite set of products (*15*).

Escherchia coli RuvC is a Holliday junction resolvase that participates in homologous recombination and recombinational repair. Genetic evidence shows that RuvC, together with the branch migration-promoting RuvA−RuvB complex, functions to restore the system to double helicity after the formation of recombinational intermediates by the RecA protein (*9*). RuvC is one of the best characterized Holliday junction resolvases. Studies on the purified protein have established its sequence specificities (*9, 16*) and the catalytic amino acids (*17*); furthermore, its crystal structure has been determined (*18*). The enzyme requires sequence symmetry, which means that its substrate is free to branch migrate. However, a large range of sequence symmetry is not required (*19*). Sequence preferences appear to be WTT|S, where the vertical bar represents the cleavage site, W is A/T and S is G/C; the cleavage sites are on the noncrossover strands (*9*, *16*), but the position of the branch point, relative to the recognition sites, is not determined by the recognition sites. Bennett and West (*20*) have attempted to ascertain this information by means of modified oligonucleotides. Here, we report a different experiment, using symmetric immobile junctions (SIJs),[1] that enables us to investigate a more complete group of possible cleavage sites; although our results are in qualitative agreement with those of Bennett and West, we find that one of the newly explored sites appears to provide a better substrate, suggesting that the preferred site of cleavage lies one nucleotide 3′ to the crossover position.

DNA double-crossover (DX) molecules contain two branch points where the strands cross over between two double-helical domains (*21*). SIJs (*22*) are DX molecules that contain one branch point flanked by a symmetric sequence and an immobile branch point nearby flanked by an asymmetric sequence. When the separation between the two crossover points is short, the symmetric branch point cannot migrate, because its relocation would increase the torque on the intervening helices. We have used SIJs to establish the crossover preferences of symmetric Holliday junctions (*13*), and the relative free energies of branch migratory minima (*23*). The ability to fix the site of a symmetric sequence enables us to construct a series of molecules with branch points fixed at individual loci. DX molecules may contain parallel or antiparallel helical domains, but the geometry around the dyad axis of RuvC suggests that antiparallel molecules are more appropriate (*18*). Consequently, we have selected the antiparallel DAO motif (Figure 2a) of DX molecules (*21*) for the symmetric immobile junctions we have used.

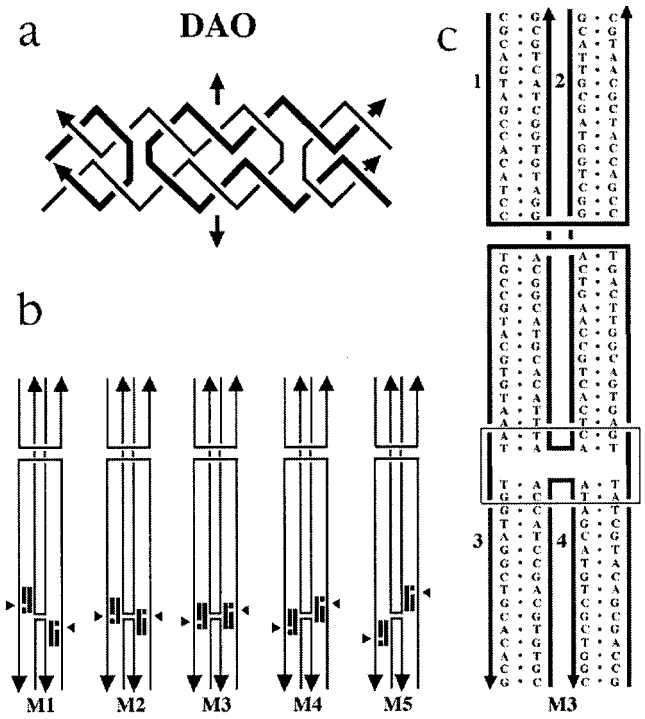

FIGURE 2: Schematic drawings of the molecules used in this study. (a) The topology of a DAO double-crossover molecule. The molecule shown here contains two double-helical domains connected by two crossover points (hence the D of its name). The helices are antiparallel (hence the A), and there is an odd number (hence the O) of double-helical half-turns between the crossover points. One of the crossover points is flanked by an asymmetric sequence, and the other is flanked by a symmetric sequence that is held immobile by torsion on the helices between the crossovers. (b) The experimental species used to establish the position of the branch point relative to the recognition sequence. The immobile junction is the upper junction in each of the five molecules, and the SIJ is the lower junction. The four-nucleotide RuvC recognition sequences, ATT|G (on the noncrossover strands) and its complement CAAT (on the crossover strands), are indicated by the pairs of black bars that flank the symmetric immobile junction. The site of cleavage between the T and the G is indicated by a gap in the black bar on the continuous strand, and also by a triangle pointing to the gap. Five molecules (M1−M5) are used; the position of the recognition sequence is completely 5′ to the junction in M1, and it moves one nucleotide in the 3′ direction in each of the succeeding molecules. (c) A representative molecule. The sequence of molecule M3 is shown in an enlarged representation. M1−M5 differ in the location of ATT|G sequence, whose positions are illustrated schematically in panel b.

Figure 2b illustrates the five primary molecules employed here. The upper crossover is the asymmetric immobile junction, and the lower crossover is the symmetric immobile junction; the vertical bars represent the cleavage sequence 5′-ATT|G-3′ on the noncrossover strands. The point of cleavage between the T and the G is indicated by a gap in the bars on the noncrossover strands, and by a triangle pointing at the gap. We have varied the position of this sequence in five single steps, starting with it 5′ to the crossover point, and ending with it 3′ to the crossover. Figure 2c shows an example of one of these molecules, M3. We have examined the cleavage of these five molecules by RuvC, and find that M3 is both the molecule with the highest V_{max}

[1] Abbreviations: DAO, antiparallel double crossover with an odd number of double-helical half-turns between crossover points; DX, double crossover; SIJ, symmetric immobile junction; TAEMg, solution containing 40 mM Tris (pH 8.0), 20 mM acetic acid, 2 mM EDTA, and 12.5 mM magnesium acetate; TBE, solution containing 100 mM Tris (pH 8.3), 89 mM boric acid, and 2 mM EDTA.

and the one that produces the greatest amount of product. We conclude that RuvC cleaves 5′-ATTG-3′ sequences when the cleavage site is one nucleotide 3′ to the crossover position.

MATERIALS AND METHODS

Design of the Substrates. The DAO molecules here resemble those used previously as SIJs (*22*), except that the outer helices are longer, to increase stability under cleavage conditions. They contain 16 nucleotide pairs on each helix in the region between the crossover points. Figure 2a shows that the backbone symmetry element is vertical in the plane of the page, suggesting that the two helices between crossovers are not equivalent. From model building (*24*), it is unclear whether both helices are minimally strained with this arrangement, or with 15 nucleotide pairs in the helix shown on the right in Figure 2c. Three molecules (M2, M3, and M5) have been built with both architectures. Sequences have been designed with the program SEQUIN (*25*), to minimize sequence symmetry (*8*).

Synthesis and Purification of DNA. All DNA molecules were synthesized on an Applied Biosystems 380B DNA synthesizer, removed from the support, and deprotected using routine phosphoramidite procedures (*26*). All strands have been purified by denaturing polyacrylamide gel electrophoresis.

Formation of Double-Crossover Molecules. The strands of the double-crossover molecules (60 pmol) were dissolved to a concentration of 3 μM in 20 μL of a solution containing 40 mM Tris (pH 8.0), 20 mM acetic acid, 2 mM EDTA, and 12.5 mM magnesium acetate (TAEMg), heated to 90 °C for 5 min, and then cooled to 65 °C for 15 min, 37 °C for 15 min, room temperature (ca. 22 °C) for 20 min, and 4 °C for 20 min. The protocol has been interrupted at the appropriate stages for experiments performed at higher temperatures.

Hydroxyl Radical Autofootprinting Analysis. Individual strands of the molecules were radioactively labeled, and were additionally gel purified from a 15% denaturing polyacrylamide gel. Each of the labeled strands (approximately 10 pmol in TAEMg) was annealed to a 4-fold excess of the unlabeled complementary strand, annealed to the complex, as described above, left untreated as a control, or treated with sequencing reagents (*27*) for a sizing ladder. Hydroxyl radical cleavage of the samples took place at 4 °C for 100 s (*28*), with modifications noted by Churchill et al. (*29*). The reaction was stopped by addition of thiourea. The samples were ethanol precipitated, dried, dissolved in a formamide/dye mixture, and loaded directly onto a 14% polyacrylamide sequencing gel containing 8.3 M urea. Autoradiograms were quantitated using a Bio-Rad GS-250 Molecular Imager.

Enzymatic Reactions. (1) Radioactive Labeling. Phosphorylation was performed as described previously (*11*).

(2) RuvC Digestions. RuvC was prepared as described previously (*17*). The DNA complex (20 pmol) at a concentration of 1 μM, annealed as described above at 37 °C, was combined with 60 pmol (3 μM) of RuvC and allowed to incubate for 45 min in 20 μL of the RuvC reaction buffer [10 mM $MgCl_2$, 1 mM dithiothreitol, 0.01% bovine serum albumin, 20 mM Tris (pH 8.0), and 5% glycerol]. The reaction was stopped by adding 2 μL of 500 mM EDTA, heating to 90 °C for 5 min, drying down, and adding 10 μL of denaturing gel loading dye.

(3) 3′ Labeling of Strands. The DNA strand and cacodylate buffer (Amersham) were thawed on ice, and reaction components were added; 5 μL of 10× cacodylate buffer [containing sodium cacodylate, cobalt chloride, and dithiothreitol (pH 7.2)], 10 pmol of DNA, 5 μL of [α-^{32}P]ddATP (10 mCi/mL, Amersham), 10 units of terminal transferase (Amersham), and water were added to a final volume of 50 μL. The solution was mixed gently by pipetting up and down in the pipet tip, and incubated for 1−2 h at 37 °C. The reaction was stopped by the addition of 5 μL of 0.5 M EDTA, and the product was purified by a polyacrylamide sequencing gel.

Polyacrylamide Gel Electrophoresis. (1) Denaturing Gels. These gels contained 8.3 M urea and were run at 55 °C. Gels contained 6 to 20% acrylamide (19:1 acrylamide:bisacrylamide ratio). As a check on mobilities, some control gels were also run containing an additional 20−40% formamide. The running buffer consisted of 100 mM Tris (pH 8.3), 89 mM boric acid, and 2 mM EDTA (TBE). The sample buffer consisted of 10 mM NaOH, 1 mM EDTA, 90% formamide, and 0.1% xylene cyanol FF tracking dye. Gels were run on an IBI model STS 45 electrophoresis unit at 70 W (50 V/cm), constant power, dried onto Whatman 3MM paper, and the distribution of each species was quantitated using a Bio-Rad GS-250 Molecular Imager.

(2) Nondenaturing Gels. Nondenaturing gels were prepared and run as described previously (*11*).

Gel Retardation Experiments. A solution containing 20 pmol (1 μM) of symmetric immobile junction, labeled on strand 3, was incubated with inactive mutant D7E of RuvC (*17*) at 4 °C for 15 min in 20 μL of RuvC binding buffer, a variant of the reaction buffer in which 1 mM $MgCl_2$ is replaced with 10 mM $MgCl_2$. Gels containing 8% acrylamide (19:1 acrylamide:bisacrylamide ratio) were buffered with 44.5 mM Tris (pH 8.0), 44.5 mM boric acid, and 1 mM EDTA. The sample buffer was the same as the running buffer, except that it contained 5% glycerol and 0.1% xylene cyanol FF tracking dye. Electrophoresis was performed on a Hoefer SE-600 unit at 4 °C for 4 h at 8.3 V/cm. The gels were pre-electrophoresed for 0.5 h under the same conditions, dried, and quantitated as described above.

Hydroxyl Radical Hypersensitivity Assay. A 20 μL solution of RuvC binding buffer containing 1 μM DNA and 3 μM D7E mutant RuvC was incubated for 10 min at 4 °C. A 6 μL aliquot was taken, and this solution was subjected to the hydroxyl radical protocol described above. In an alternative procedure, the 4 °C sample was warmed to 37 °C, incubated for 15 min, subjected to the hydroxyl radical protocol, and then analyzed by gel.

RESULTS

Nondenaturing Gel Electrophoretic Characterization of Substrates. Figure 3 illustrates a nondenaturing gel containing all of the five molecules indicated in Figure 2b. In addition, we also show two other species, M3′ and M5′, containing 15 nucleotide pairs in their right domain (see Design of Substrates). As with previous work (*21*), we interpret a lane containing a single band with approximately the expected mobility as evidence of a stable molecular complex. Other

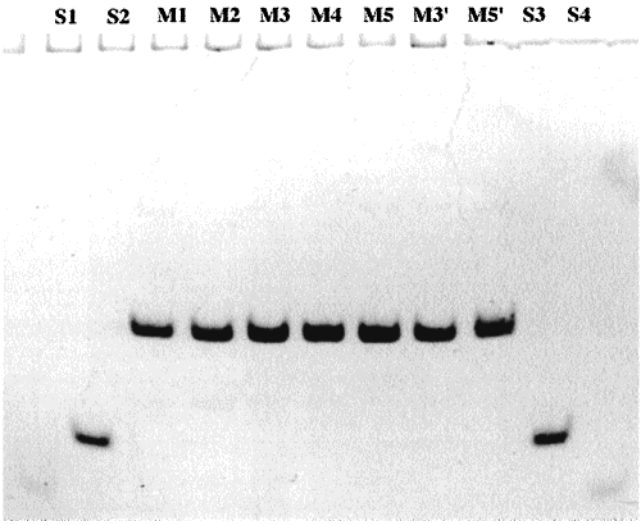

FIGURE 3: Nondenaturing gel with the molecules used here. The image is of an 8% gel run at 4 °C. S1−S4 represent the four strands of one molecule (S1 and S4 are very faint). M1−M5 represent the five experimental molecules, and M3′ and M5′ represent variants of molecules M3 and M5, respectively. In each case, a single molecular band is seen, with neither lower bands (indicating decomposition) nor upper bands (indicating strain) present.

than the target complexes, no other electrophoretic species are visible on this gel. Thus, the DAO molecules are all stable complexes in which every strand participates. This gel has been run at 4 °C, but it looks identical to a gel run at 37 °C (data not shown).

Hydroxyl Radical Autofootprinting of the Symmetric Branch Point Position. We have used hydroxyl radical autofootprinting previously to characterize unusual DNA molecules, including branched junctions (*29*), antijunctions and mesojunctions (*30*), and double-crossover molecules (*11*, *21*), including SIJs (*13*, *22*, *23*). These experiments are performed by labeling a component strand of the complex and exposing it to hydroxyl radicals. The key feature noted at crossover sites is a decreased susceptibility to attack when comparing the pattern of the strand as part of the complex relative to the pattern of the strand when it is paired to its conventional Watson−Crick complement in linear duplex DNA. Decreased susceptibility suggests that access of the hydroxyl radical is limited by steric factors (*31*). In previous studies of junctions and DX molecules, protection has been seen particularly at the two nucleotides flanking the crossover sites and the nucleotide 5′ to them. Hence, crossover sites can be located reliably by hydroxyl radical autofootprinting analysis.

The position of the crossover point of the symmetric immobile junction is established by the protection pattern on strands 3 and 4, whose patterns are similar at the crossover points. The autofootprinting data for strand 4 at 37 °C are illustrated in Figure 4 for M1−M5, and for variants of molecules M2, M3, and M5 in which the right helix (Figure 2) contains 15 nucleotide pairs. For each of the molecules M1−M4, the data in Figure 3 indicate that the major sites of protection are the two nucleotides flanking the branch point and the nucleotide 5′ to it. This is not the case for molecule M5, whose protection pattern is shifted one nucleotide 5′ to the expected pattern. The variant of M5, M5′, corrects this problem and has been used along with M5. The variants of M2 and M3 were constructed as controls.

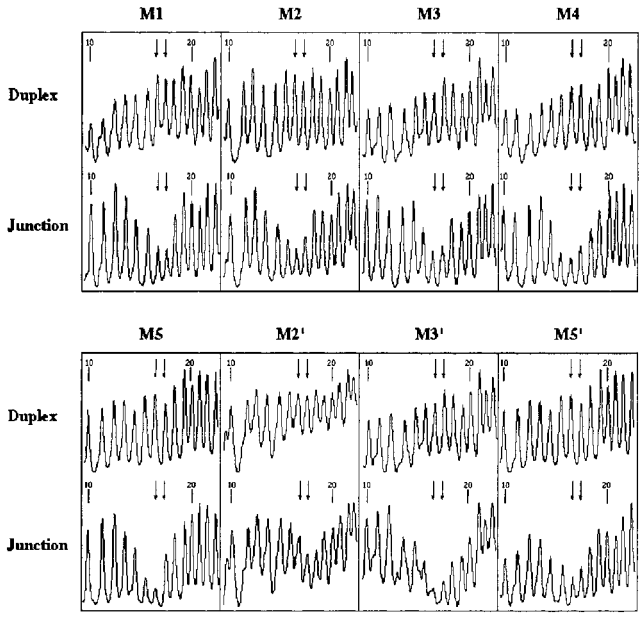

FIGURE 4: Hydroxyl radical autofootprinting data. Each panel represents the extent of cleavage of strand 4 of the indicated molecule. The cleavage pattern is compared for the strand when it is a component of the DAO symmetric immobile junction complex (labeled Junction) and when it is complexed with its Watson−Crick complement in a double-stranded structure (labeled Duplex). The numbering of the strand is indicated; the key points are positions 16 and 17, which flank the crossover (arrows pointing downward).

The M2′ molecule shows a pattern shifted 3′ to the expected pattern, and the M3′ molecule shows a pattern similar to the pattern of M3. The M2′ molecule was not used further, except for gel retardation. The autofootprinting data for the other three strands of each of these molecules are similar to patterns seen previously for SIJs (*13*, *22*, *23*; data not shown). The data show conclusively that we have produced immobile branched junctions with symmetric sequences at the designated loci for each of the molecules M1−M4, and M5′.

Cleavage of Symmetric Immobile Junctions by RuvC. Figure 5 shows the products of RuvC cleavage of strand 3 of each of the substrates. Figure 5a shows the products of 5′ labeling and Figure 5b the products of 3′ labeling, so both cuts are shown. In each case, the sequence specificity of RuvC dominates over structure so that scission occurs at the same position, between T and G. The cleavage sites have been checked by using 40% formamide gels, to be sure that the products are sufficiently denatured. In both cases, the rank order of the extent of digestion is the same: M3 > M2 > M4 > M1 > M5′.

A quantitative picture of cleavage is illustrated in Figure 5c, which shows the reaction kinetics, based on the cleavage of the 5′-labeled strand. Molecule M3 has the highest initial velocity and also produces the most product. Molecule M2 is somewhat behind M3, followed by M4, M1, M3′, M5 (higher initial rate than M3′, but less ultimate product), and M5′. The initial rates and errors measured for the molecules are, in decreasing order, as follows: M3, 0.053, 0.005; M2, 0.040, 0.003; M4, 0.030, 0.004; M1, 0.015, 0.002; M5, 0.013, 0.001; M3′, 0.010, 0.002; and M5′, 0.005, 0.001. In control experiments, we have ensured that the labeled strand is in the complex, by using a 2:1 ratio of unlabeled to labeled strands in the reaction. Under these conditions, M3 is an even better substrate for RuvC (data not shown).

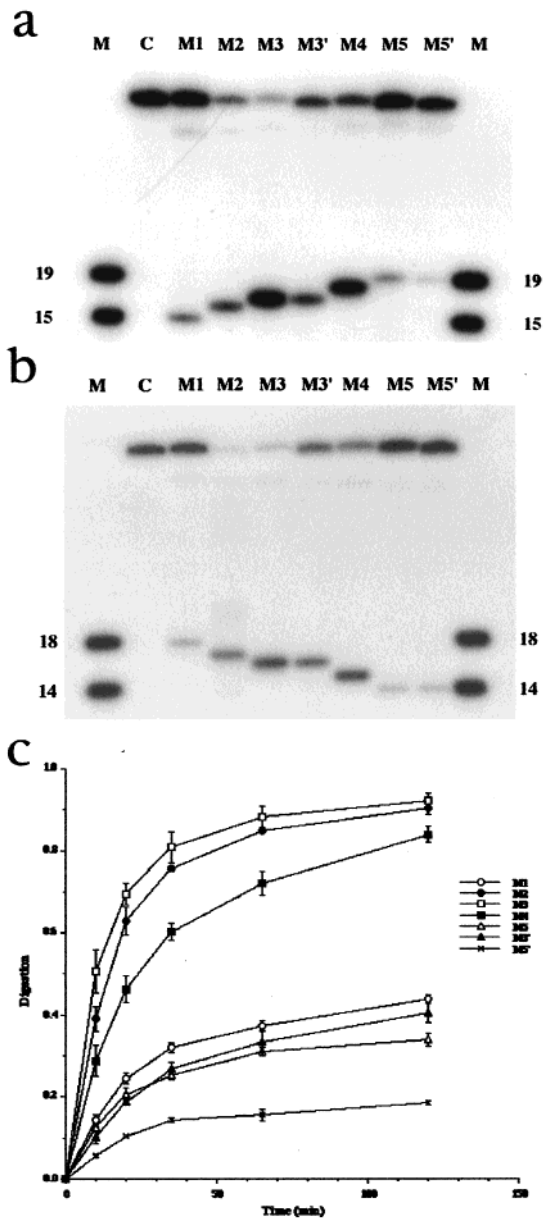

FIGURE 5: Cleavage of symmetric immobile junctions by RuvC. (a) The products of cleavage for 5′ labeling of strand 3. This is an autoradiogram of a 20% denaturing gel. M represents a pair of markers, 19 and 15 nucleotides long; C represents an unreacted control. (b) The products of cleavage for 3′ labeling of strand 3. The same conventions apply here as for panel a. (c) The course of the digestion. The extent of digestion is monitored for seven SIJs. Note that both the initial rate and the extent of digestion are highest for molecule M3.

Gel Retardation of SIJs by RuvC. We have analyzed the binding of RuvC to substrate by means of gel retardation assays using a site-directed mutant (D7E) that can bind DNA, but not cleave it. Figure 6 shows the results of a binding assay both run and electrophoresed at 37 °C. Each molecule contains two Holliday junctions; therefore, there are two binding sites, and two bands are evident for each substrate. RuvC does not have a sequence preference for binding (*16*, *32*), so the lower level of second binding seen for M5′ may be due to its unusual intercrossover spacing.

Hydroxyl Radical Hypersensitivity. The binding of RuvC to the substrate produces sites hypersensitive to hydroxyl radicals at the two nucleotides 3′ to the crossover point on the noncrossover strands of immobile junctions (*33*). We

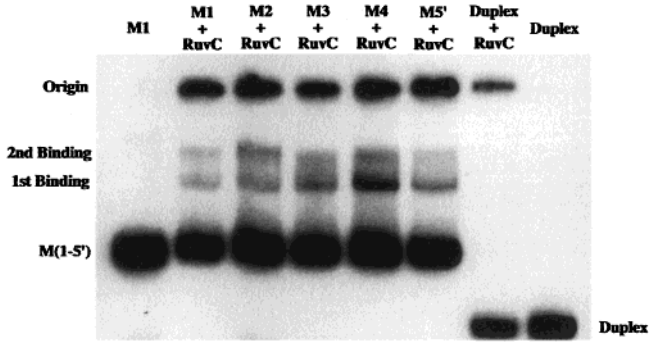

FIGURE 6: Gel retardation of SIJs by RuvC at 37 °C. This is an autoradiogram of an 8% nondenaturing gel. A control lane containing M1, but lacking RuvC, is shown on the left. Strand 3 is labeled in all molecules. The right side of the gel contained duplex controls, one with RuvC, and one without it; the duplex molecule is strand 3 of M3 and its Watson−Crick complement. The two bindings are indicated at the left of the gel.

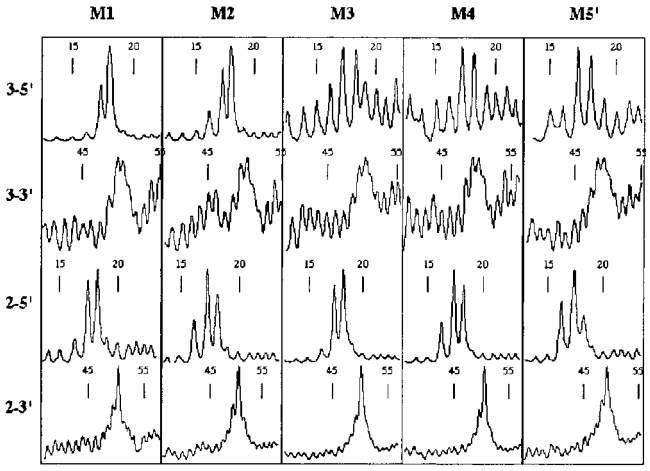

FIGURE 7: Hydroxyl radical hypersensitivity. The five molecules with the most reliable autofootprints on strand 4 (see Figure 4) are examined. Strands 2 and 3 are shown, because they contain the noncrossover strands for both junctions. The cleavage pattern for each strand has been broken up into two parts. The key nucleotides for the SIJ are nucleotides 17 and 18 on the 5′ end of strand 3 and nucleotides 49 and 50 on the 3′ end of strand 3, except for M5′ (one nucleotide shorter), where they are nucleotides 48 and 49. In each case, these are the maximally cleaved residues. As a control, the same data are shown for the immobile junction. In this case, the key residues are nucleotides 17 and 18 on the 5′ end of strand 2 and nucleotides 49 and 50 on the 3′ end of strand 2, again with the exception of M5′, where they are nucleotides 48 and 49. Again, the proper nucleotides are hypersensitive, except for M5′, where the major sites are nucleotides 16 and 17, possibly due to the distortions resulting from the shorter helix.

have used inactive mutant D7E to perform hypersensitivity experiments on substrates M1−M4 and M5′ (Figure 7). The primary sites of hypersensitivity exist on the helical strands. Both branch points are sensitive, the one containing the symmetric immobile site (strand 3) and the one containing the immobile site (strand 2). Regardless of sequence, hypersensitivity is seen primarily on the noncrossover strand, two nucleotides 3′ to the branch point; these are sites 17 and 18 or 49 and 50 (48 and 49 in M5′). Sometimes, the signal-to-noise ratio is poor, and sometimes, other sites are almost as heavily cleaved. In the cases of strand 2 on molecules M4 and M5′, the positions of maximal cleavage are shifted one nucleotide in the 5′ direction. A small hypersensitivity signal is also seen in the immobile junction

on the nucleotide 5′ to the immobile junction on strand 2 (5′ portion) in molecules M2, M4, and (somewhat larger) M5′; another small hypersensitivity signal is seen in M2 on the nucleotide 5′ to the SIJ on strand 3 (5′ portion).

DISCUSSION

Characterization of the SIJs. The SIJs have been shown to be stable species whose branch points are forced to remain at the designated positions. The one exception, M5, has been modeled in a molecule containing 15 nucleotide pairs in one of its arms, M5′. One possible objection to the use of SIJs of this type is that the helix axes are constrained to be coplanar. The angle between the helices is known to be 60° for immobile branched junctions in solution (*34*−*36*), and a docking experiment of a Holliday junction with RuvC (*18*) also suggests significant distortion. This feature may delay the enzyme in producing the active intermediate. Variations of catalytic rates may represent the time taken for RuvC to distort the SIJ; likewise, rate variations may represent the frequency of fluctuation structures closest to the authentic intermediate used by the enzyme. Nevertheless, each of the molecules must undergo the same distortions, so a comparison between them is likely to give a good indication of the actual substrate.

Interaction of RuvC with the SIJ. The rates of catalysis indicate that molecule M3 is the most effective substrate, markedly better than M2 or M4. In every case, cleavage occurs at the same site, between the T and the G of the symmetric sequence, regardless of its position relative to the branch point. Hence, the efficacy of catalysis can be regarded as a measure of bringing the TpG linkage into the proper position for cleavage. M3 is the molecule whose TpG linkage is one nucleotide 3′ to the crossover position. Regardless of the nature of the rate-limiting step, the distortion of the substrate, or the frequency of appropriately structured fluctuations, the cleavage data show that the position one nucleotide 3′ to the crossover point functions most effectively as the site of cleavage.

It is a useful control to characterize equilibrium binding structures to complement cleavage data. An enzyme may process rare fluctuations, but equilibrium data represent the bulk of the molecules present. The gel retardation data suggest that binding is not the rate-limiting step in this system (Figure 6), because the binding is qualitatively similar for M1−M4. This finding is in agreement with previous studies which showed that binding to the junction is independent of sequence (*19*, *32*, *33*). The RuvC mutant binds poorly to M5, M2′, M3′, and M5′, molecules in which the two helical domains may be distorted, suggesting that a simple arrangement of 16 nucleotide pairs in each helical domain is most relaxed. The sequence at the branch point is the same in M3 and M3′, but model building (*24*) suggests that the structures of their branch points are likely to be substantially different, thus accounting for the differences seen in binding and cleavage data.

A more telling equilibrium analysis is the hydroxyl radical hypersensitivity experiment. Regardless of sequence for M1−M4, the primary sites of hypersensitivity are the two nucleotides that flank the internucleotide linkage one position 3′ to the crossover point on the noncrossover strands. These data are in agreement with the hydroxyl radical autofootprinting data. This observation is true for both junctions, the SIJ and the immobile junction on the other end of the molecule. Occam's razor would suggest that the hypersensitivity is a consequence of distorting the target dinucleoside by RuvC, preliminary to cleavage; if true, then the hypersensitivity data are in agreement with our suggestion that this linkage is the site of RuvC activity.

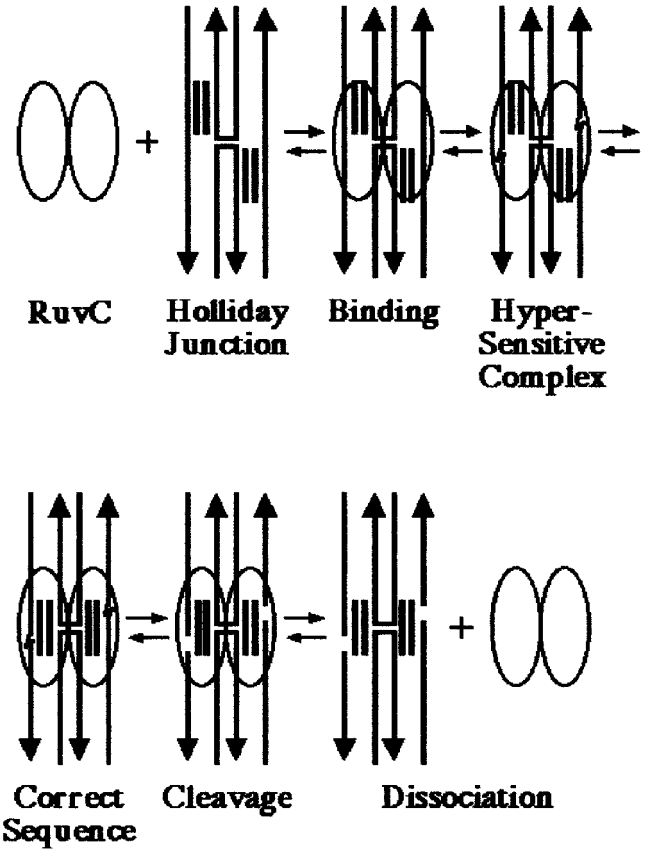

FIGURE 8: Steps in the cleavage of Holliday junctions by RuvC. The first step shown is binding, which the data here suggest is not rate-limiting. This is followed by the formation of the hypersensitive complex, although we cannot exclude the possibility that this step and the previous one occur simultaneously. The third step entails positioning the right sequence into the site. Such a step must exist, because we have demonstrated that unfavored sequences also can form the hypersensitive complex. Cleavage and dissociation follow the placement of the correct sequence into the active site.

The conclusion drawn here differs from that reached by Bennett and West (*20*). Their system is predicated on the immobilization of symmetric junctions by the introduction of methyl phosphonates. Their analysis of the constructs they made excluded the equivalents of molecules M3 and M4 as being inappropriate for continued experiments, because those molecules did not fix the branch point at a single site. Consequently, the favored site in our experiments was outside the window of their analysis. Our results agree with theirs in the order of substrate quality: M2 > M1 > M5.

Model for the Enzymatic Mechanism. The data presented here lead to a model of the steps involved in the catalysis of junction resolution by RuvC in vitro. The model must explain the following points known from the data above and from previous work: (1) RuvC binds to four-arm junctions in a sequence-independent fashion; (2) RuvC induces hypersensitivity to hydroxyl radicals, which may be important for proper orientation of the DNA, but is insufficient for nicking;

and (3) RuvC demonstrates a clear sequence preference for cleavage.

A model to account for these properties is illustrated in Figure 8. This diagram shows that the first step, probably not rate-limiting, is the binding of RuvC to the junction. The formation of the hypersensitive complex occurs next, although we cannot exclude the possibility that it is an inherent component of the binding step. For the complex to be productive, the active site of RuvC must contain an appropriate sequence, and achieving this state is the next step. In a system free to migrate, binding to the proper sequence may occur by branch migration; proper resolution by RuvC in vivo is known to require the RuvA−RuvB branch migratory system (*38*). It is likely that the nature of the transformation in the system used here entails other structural changes; regardless of the structural nature of the changes needed to position the cleavage site on the surface of RuvC, the data presented here suggest that this step is likely to be rate-determining. Once the productive complex is obtained, catalysis can proceed to yield resolved products. We expect experiments with more sophisticated symmetric immobile junctions suggested recently (*37*) to lead to further insight into the mechanism of RuvC.

ACKNOWLEDGMENT

N.C.S. thanks the Institut des Hautes Études Scientifiques in Bures-Sur-Yvette, France, for its hospitality during the writing of the manuscript.

REFERENCES

1. Holliday, R. (1964) *Genet. Res. 5*, 282−304.
2. Hoess, R., Wierzbicki, A., and Abremski, K. (1987) *Proc. Natl. Acad. Sci. U.S.A. 84*, 6840−6844.
3. Kitts, P. A., and Nash, H. A. (1987) *Nature 329*, 346−348.
4. Nunes-Duby, S. E., Matsumoto, L., and Landy, A. (1987) *Cell 50*, 779−788.
5. DasGupta, C., Wu, A. M., Kahn, R., Cunningham, R. P., and Radding, C. M. (1981) *Cell 25*, 507−516.
6. Lilley, D. M. J., and Clegg, R. M. (1993) *Annu. Rev. Biophys. Biomol. Struct. 22*, 299−328.
7. Seeman, N. C., and Kallenbach, N. R. (1994) *Annu. Rev. Biophys. Biomol. Struct. 23*, 53−86.
8. Seeman, N. C. (1982) *J. Theor. Biol. 99*, 237−247.
9. Shinagawa, H., and Iwasaki, H. (1996) *Trends Biochem. Sci. 21*, 107−111.
10. Hsieh, P., and Panyutin, I. G. (1995) *Nucleic Acids Mol. Biol. 9*, 42−65.
11. Li, X., Wang, H., and Seeman, N. C. (1997) *Biochemistry 36*, 4240−4247.
12. Miick, S. M., Fee, R. S., Millar, D. P., and Chazin, W. J. (1997) *Proc. Natl. Acad. Sci. U.S.A. 94*, 9080−9084.
13. Zhang, S., and Seeman, N. C. (1994) *J. Mol. Biol. 238*, 658−668.
14. Mueller, J. E., Kemper, B., Cunningham, R. P., Kallenbach, N. R., and Seeman, N. C. (1988) *Proc. Natl. Acad. Sci. U.S.A. 85*, 9441−9445.
15. Bennett, R. J., and West, S. C. (1995) *Proc. Natl. Acad. Sci. U.S.A. 92*, 5635−5639.
16. Shah, R., Bennett, R. J., and West, S. C. (1994) *Cell 79*, 853−864.
17. Saito, A., Iwasaki, H., Ariyoshi, M., Morikawa, K., and Shinagawa, H. (1995) *Proc. Natl. Acad. Sci. U.S.A. 92*, 7470−7474.
18. Ariyoshi, M., Vassylyev, D. G., Iwasaki, H., Nakamura, H., Shinagawa, H., and Morikawa, K. (1994) *Cell 78*, 1063−1072.
19. Shida, T., Iwasaki, H., Saito, A., Kyogoku, Y., and Shinagawa, H. (1996) *J. Biol. Chem. 271*, 26105−26109.
20. Bennett, R. J., and West, S. C. (1996) *Proc. Natl. Acad. Sci. U.S.A. 93*, 12217−12222.
21. Fu, T.-J., and Seeman, N. C. (1993) *Biochemistry 32*, 3211−3220.
22. Zhang, S., Fu, T.-J., and Seeman, N. C. (1993) *Biochemistry 32*, 8062−8067.
23. Sun, W., Mao, C., Liu, F., and Seeman, N. C. (1998) *J. Mol. Biol. 282*, 59−70.
24. Seeman, N. C. (1988) *J. Biomol. Struct. Dyn. 5*, 997−1004.
25. Seeman, N. C. (1990) *J. Biomol. Struct. Dyn. 8*, 573−581.
26. Caruthers, M. H. (1985) *Science 230*, 281−285.
27. Maxam, A. M., and Gilbert, W. (1980) *Methods Enzymol. 65*, 499−560.
28. Tullius, T. D., and Dombroski, B. A. (1985) *Science 230*, 679−681.
29. Churchill, M. E. A., Tullius, T. D., Kallenbach, N. R., and Seeman, N. C. (1988) *Proc. Natl. Acad. Sci. U.S.A. 85*, 4653−4656.
30. Du, S. M., Zhang, S., and Seeman, N. C. (1992) *Biochemistry 31*, 10955−10963.
31. Balasubramanian, B., Pogozelski, W. K., and Tullius, T. D. (1998) *Proc. Natl. Acad. Sci. U.S.A. 95*, 9738−9743.
32. Takahagi, M., Iwasaki, H., and Shinagawa, H. (1994) *J. Biol. Chem. 269*, 15132−15139.
33. Bennett, R. J., Dunderdale, H. J., and West, S. C. (1993) *Cell 74*, 1021−1031.
34. Murchie, A. I. H., Clegg, R. M., von Kitzing, E., Duckett, D. R., Diekmann, S., and Lilley, D. M. J. (1989) *Nature 341*, 763−766.
35. Eis, P. S., and Millar, D. P. (1993) *Biochemistry 32*, 13852−13860.
36. Mao, C., Sun, W., and Seeman, N. C. (1999) *J. Am. Chem. Soc. 121*, 5437−5443.
37. Sha, R., Liu, F., Bruist, M. F., and Seeman, N. C. (1999) *Biochemistry 38*, 2832−2841.
38. Mandal, T. N., Mahdi, A. A., Sharples, G. J., and Lloyd, R. G. (1993) *J. Bacteriol. 175*, 4325−4334.

BI001037Z